Downloaded from rsta.royalsocietypublishing.org

A Study of 5p Excitation in Atomic Barium: II. A Fully Relativistic Analysis of 5p Excitation in Atomic Barium

S. J. Rose, I. P. Grant and J. P. Connerade

Phil. Trans. R. Soc. Lond. A 1980 **296**, 527-544
doi: 10.1098/rsta.1980.0191

Email alerting service Receive free email alerts when new articles cite this article - sign up in the box at the top right-hand corner of the article or click **here**

To subscribe to *Phil. Trans. R. Soc. Lond. A* go to: **http://rsta.royalsocietypublishing.org/subscriptions**

This journal is © 1980 The Royal Society

Downloaded from rsta.royalsocietypublishing.org

A STUDY OF 5p EXCITATION IN ATOMIC BARIUM
II. A FULLY RELATIVISTIC ANALYSIS OF 5p EXCITATION IN ATOMIC BARIUM†

By S. J. ROSE‡, I. P. GRANT‡ and J. P. CONNERADE||
‡ *Department of Theoretical Chemistry*, 1 *South Parks Road, Oxford OX*1 3*TG, U.K.*
|| *Blackett Laboratory, Imperial College, Prince Consort Road, London SW*7 2*AZ, U.K.*
and Physikalisches Institut, Universität Bonn, 53 *Bonn, West Germany*

(*Communicated by W. R. S. Garton, F.R.S. – Received* 5 *December* 1978 – *Revised* 30 *April* 1979)

[Plate 1]

A fully relativistic *ab-initio* multiconfiguration Dirac–Fock (m.D.–F.) procedure has been used to identify six prominent peaks in the 5p electron-impact ionization spectrum of Ba I and thereby also suggest assignments for each series limit in the 5p-photo-absorption (synchrotron radiation) spectrum of Ba I.

Comparison between single configuration m.D.–F. and non-relativistic H.–F. intermediate coupling calculations show differences in the predicted ordering of levels; triple manifold m.D.–F. calculations show the interaction between configurations $5p^5\,6s^2$, $5p^5\,5d\,6s$ and $5p^5\,5d^2$ of Ba II to be responsible for the prominence of supernumerary excitations in each experiment.

1. Introduction

The spectrum of 5p-excited Ba I has attracted much interest in recent years: anomalies concerning the Ba^{2+}/Ba^{+} photoionization rates were found by Brehm & Bucher (1974) and Hotop & Mahr (1975). Several explanations have been proposed: Fano (1973) has discussed collective effects (cf. Wendin 1974); Wendin (1978) has proposed a mechanism relying on near-resonance direct photoemission to Ba^{+} followed by Auger emission; and Hansen (1975 *a*) has proposed an explanation ('two-step autoionization') within the framework of the independent particle model which relies on the coincidence of the He I resonance line with an absorption line in the 5p-spectrum of Ba I.

Collective effects in the form of 'giant' resonances, which were predicted by Wendin (1974) to arise from (5p; *n*d) intrachannel coupling in Ba I, have been investigated experimentally by Connerade *et al.* (1974) whose results did not conform closely to the theory. Subsequent studies of 5p-excitation from Ba to Yb (Connerade & Tracy 1977) suggested that the 'giant' resonance in Ba I is diluted by the effect of 6s–5d mixing.

More recently Connerade *et al.* (1979 *a*) have presented a detailed study of the 5p-spectrum of Ba I. The spectrum has been classified into series converging onto 12 levels of Ba II, the energies of which are in close correspondence with binding energy measurements for the 5p shell of Ba I obtained by Mehlhorn *et al.* (1977) by electron-impact spectroscopy (figure 1). According to a simple one-electron model, only two Ba II levels, $5p^5\,6s^2\,{}^2P_{\frac{1}{2}}$ and ${}^2P_{\frac{3}{2}}$, should be involved in both cases, yet the experiments reveal a much richer structure.

---

† Part I appeared in *Phil. Trans. R. Soc. Lond.* A **290**, 327–352.

PHILOSOPHICAL TRANSACTIONS OF THE ROYAL SOCIETY A MATHEMATICAL, PHYSICAL & ENGINEERING SCIENCES
PHILOSOPHICAL TRANSACTIONS OF THE ROYAL SOCIETY A MATHEMATICAL, PHYSICAL & ENGINEERING SCIENCES
The Royal Society is collaborating with JSTOR to digitize, preserve, and extend access to *Philosophical Transactions of the Royal Society of London. Series A, Mathematical and Physical Sciences.* www.jstor.org

Downloaded from rsta.royalsocietypublishing.org

In this paper an *ab-initio* multiconfiguration self-consistent-field Dirac–Fock (m.D.–F. procedure (Grant *et al.* 1976) is applied to the interpretation of both sets of experimental results. These calculations allow for 6s–5d mixing as well as the inclusion of relativistic effects. Connerade *et al.* (1979*a*) suggest that the appearance of more than two series is due to 6s–5d mixing in the Ba II ion. This suggestion originated (Connerade & Mansfield 1974) from a comparison with 5p-excitation in the Cs I spectrum (Connerade 1970). Rose *et al.* (1978) applied the m.D.–F. method to the low-lying even-parity levels of Ba I, and agreement with experimental term splittings suggested that a fully relativistic treatment of the 5p-excitation in Ba I should be undertaken.

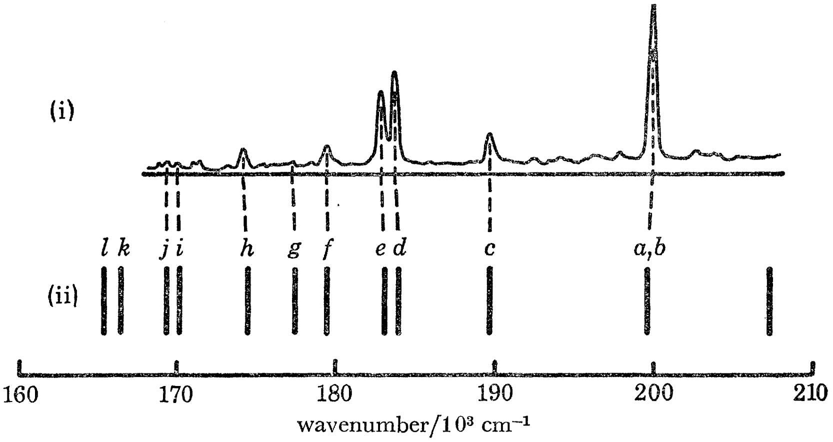

FIGURE 1. (i) Experimental Ba I 2 keV electron-impact 5p-ionization spectrum of Mehlhorn *et al.* (1977); the major peak is taken to be coincident with series limit (*a*, *b*) in the 5p photoabsorption spectrum. (ii) Experimental Ba I 5p-photoabsorption series limits (Connerade *et al.* 1979*a*). (The labels (*a*–*l*) are those given in that paper).

2. THE m.D.–F. METHOD APPLIED TO Ba II

The m.D.–F. method has already been described by Grant *et al.* (1976) and only a résumé is presented here. The wavefunction for an atomic state α is approximated by an atomic state function (a.s.f.)

$$\Psi_\alpha(PJM) = \sum_r c_{r\alpha}\,\Phi(\gamma_r PJM), \tag{1}$$

which is a linear combination of configuration state functions (c.s.f.) $\Phi(\gamma_r PJM)$, each of which corresponds to a pure *jj*-coupled state. Each c.s.f. is constructed from Dirac central-field orbitals and has total angular momentum quantum numbers J and M, and parity P, while the labels γ_r are sufficient to distinguish between different states of the same configuration and the different configurations to be included in the sum.

The orbitals used to construct the a.s.f. were determined solely by the a.l. (average level) procedure; this involves a variational calculation based on an energy functional which is the average energy of all c.s.fs with a common value of J included in the sum (1). The levels found in this way are usually within 200 cm⁻¹ of those of the corresponding (optimal) level-by-level (o.l.) m.D.–F. procedure (Grant *et al.* 1976; Rose *et al.* 1978), although this would have proved far too expensive in computer time for use on the present problem. The e.a.l. (extended average level) version, which uses the same orbital set to describe atomic states of more than one value of J, would require too much computer store to be used.

Downloaded from rsta.royalsocietypublishing.org

3. Energy levels and configuration mixing coefficients

The manifolds $5p^5\,6s^2$, $5p^5\,5d6s$ and $5d^2\,5p^5$ of Ba II were chosen for study since the large number of observed Ba II levels in photoabsorption (Connerade *et al.* 1979*a*) and electron-impact ionization experiments (Mehlhorn *et al.* 1977) (figure 1) was expected to arise from mixing between these configurations. Tables 1 and 2 show the m.D.–F. – a.l. single-manifold energy levels and mixing coefficients in *LS*-coupling* together with the corresponding results of single configuration non-relativistic Hartree–Fock average of configuration calculations with full intermediate coupling (Connerade & Mansfield 1978). For the $5p^5\,5d6s$ configuration the ordering of levels predicted by the two methods is the same and the energy splittings are similar. However, for the $5d^2\,5p^5$ levels an unambiguous designation cannot always be made on the basis of largest weight. For a particular level the eigenvectors for each method show similarities, to the extent that differences in the ordering of levels can be seen: the m.D.–F. eigenvectors for the $5d^2\,5p^5\ J = \frac{3}{2}$ levels 5, 6, 9 and 10 are taken to correspond to the H.–F. $5d^2\,5p^5\ J = \frac{3}{2}$ levels 6, 5, 10 and 9 respectively.

Table 1*a*. Energy levels for configuration $5p^5\,6s^2$

m.D.–F. single manifold‡		H.–F. average of configuration plus intermediate coupling†	
designation	energy level/cm^{-1}	designation	energy level/cm^{-1}
$^2P_{\frac{3}{2}}$	144 050	$^2P_{\frac{3}{2}}$	147 047
$^2P_{\frac{1}{2}}$	161 572	$^2P_{\frac{1}{2}}$	161 651

† J. P. Connerade & M. W. D. Mansfield (1978, private communication).

‡ Relative to single manifold m.D.–F. $5p^6 6s\ ^2S_{\frac{1}{2}}$ having a total energy of -8135.8222699 atomic units. (The atomic unit of energy is $2hcR_\infty = 27.21$ eV.)

Table 1*b*. Energy levels for configuration $5p^5\,5d\,6s$

m.D.–F.–a.l. single manifold§		H.–F. average of configuration plus intermediate coupling†	
designation	energy level/cm^{-1}	designation	energy level/cm^{-1}
$^4P_{\frac{1}{2}}$	126 674	$^4P_{\frac{1}{2}}$	121 516
$(^3P)\,^2P_{\frac{1}{2}}$	135 229	$(^3P)\,^2P_{\frac{1}{2}}$	127 845
$^4D_{\frac{1}{2}}$	150 387	$^4D_{\frac{1}{2}}$	144 185
$(^1P)\,^2P_{\frac{1}{2}}$	184 097	$(^1P)\,^2P_{\frac{1}{2}}$	173 613‡ 189 042
$^4P_{\frac{3}{2}}$	128 314	$^4P_{\frac{3}{2}}$	123 248
$(^3P)\,^2P_{\frac{3}{2}}$	137 655	$(^3P)\,^2P_{\frac{3}{2}}$	131 453
$^4F_{\frac{3}{2}}$	138 400	$^4F_{\frac{3}{2}}$	133 436
$^4D_{\frac{3}{2}}$	150 994	$^4D_{\frac{3}{2}}$	144 915
$(^1D)\,^2D_{\frac{3}{2}}$	152 818	$(^1D)\,^2D_{\frac{3}{2}}$	146 220
$(^3D)\,^2D_{\frac{3}{2}}$	159 934	$(^3D)\,^2D_{\frac{3}{2}}$	152 363
$(^1P)\,^2P_{\frac{3}{2}}$	189 266	$(^1P)\,^2D_{\frac{3}{2}}$	174 135‡ 189 255

† J. P. Connerade & M. W. D. Mansfield (1978, private communication).

‡ Separately optimized calculation (J. P. Connerade & M. W. D. Mansfield (1978, private communication)).

§ Relative to single-manifold m.D.–F. $5p^6 6s\ ^2S_{\frac{1}{2}}$.

---

* The coefficients obtained directly from the calculations are in a *jj*-basis and these have been transformed to an *LS*-basis by a transformation matrix derived by numerical diagonalization of the Hamiltonian matrix in each coupling scheme.

Downloaded from rsta.royalsocietypublishing.org

TABLE 1c. ENERGY LEVELS FOR THE CONFIGURATION $5d^2\,5p^5$

m.D.–F.–a.l. single manifold		H.–F. average of configuration plus intermediate coupling	
designation†	energy level/cm^{-1}	designation†	energy level/cm^{-1}
$(^3F)^4D_{\frac{1}{2}}$	126 602	$(^3F)^4D_{\frac{1}{2}}$	115 072
$(^3P)^2D_{\frac{1}{2}}$	138 890	$(^3P)^4P_{\frac{1}{2}}$	127 197
$(^1D)^2P_{\frac{1}{2}}$	141 952	$(^1D)^2P_{\frac{1}{2}}$	131 233
$(^3P)^4D_{\frac{1}{2}}$	156 526	$(^3P)^4D_{\frac{1}{2}}$	144 268
$(^3P)^2S_{\frac{1}{2}}$	161 332	$(^3P)^2S_{\frac{1}{2}}$	149 414
$(^3P)^2P_{\frac{1}{2}}$	174 463	$(^1S)^2P_{\frac{1}{2}}$	163 081
$(^1S)^2P_{\frac{1}{2}}$	188 749	$(^3P)^2P_{\frac{1}{2}}$	180 966
$(^3F)^4D_{\frac{3}{2}}$	127 348	$(^3F)^4D_{\frac{3}{2}}$	115 555
$(^3P)^4P_{\frac{3}{2}}$	136 575	$(^3P)^4P_{\frac{3}{2}}$	125 091
$(^3P)^4P_{\frac{3}{2}}$	137 722	$(^3F)^4F_{\frac{3}{2}}$	126 514
$(^3F)^4F_{\frac{3}{2}}$	142 528	$(^3F)^4F_{\frac{3}{2}}$	131 053
$(^3P)^2D_{\frac{3}{2}}$	150 582	$(^1D)^2D_{\frac{3}{2}}$	138 654
$(^3P)^2P_{\frac{3}{2}}$	151 213	$(^3P)^4D_{\frac{3}{2}}$	140 060
$(^3P)^4S_{\frac{3}{2}}$	158 635	$(^3P)^2D_{\frac{3}{2}}$	147 072
$(^3P)^4S_{\frac{3}{2}}$	161 268	$(^3P)^4S_{\frac{3}{2}}$	149 352
$(^1D)^2P_{\frac{3}{2}}$	164 057	$(^1S)^2P_{\frac{3}{2}}$	153 806
$(^1S)^2P_{\frac{3}{2}}$	189 976	$(^3P)^2P_{\frac{3}{2}}$	183 168
$(^3F)^2D_{\frac{3}{2}}$	192 863	$(^3F)^2D_{\frac{3}{2}}$	186 540

† The largest contribution to the particular eigenvector.
‡ Relative to single-manifold m.D.–F. $5p^6 6s\,^2S_{\frac{1}{2}}$.

No Hartree–Fock calculation allowing for interaction between the different configurations was performed by Connerade & Mansfield (1978) and, as the m.D.–F. method is suited to such calculations, an a.l. triple-manifold calculation was performed for the full set of $J = \frac{1}{2}$ and $\frac{3}{2}$ levels The resulting energies and configuration mixing coefficients are shown in table 3. The three configurations in the single-manifold calculations are found to overlap in energy and, although the spread of energies is not greatly affected, the mixing coefficients reveal considerable coupling between all three configurations to the extent that designations (such as were made in table 1) have not been proposed in table 3. Alternative labelling procedures were not found to be useful. For example the $J = \frac{3}{2}$ levels 6 and 7 each have their largest contribution from $5p^5\,6s^2\,{}^2P_{\frac{3}{2}}$ (level 6: -0.4930 (24 %), level 7: -0.6406 (41 %)), and with the common procedure whereby the level with smaller weight is designated the unassigned *LS* state with the next largest contribution, level 6 would have to be designated $(5p^5\,5d\,^3P)\,6s\,^4D_{\frac{3}{2}}$ although this assignment has a purity of only 0.1125 and the designation does not therefore have much physical significance.

Hansen (1974) presented H.–F. calculations on the two levels $(5p^5\,5d\,^3P)6s\,^2P$ and $(5p^5\,5d\,^1P)6s\,^2P$ of Ba II in which each level was optimized separately. The term dependence of the 5d orbital and associated parameters was very marked. Since the present m.D.–F.–a.l. calculations use a common set of orbitals for each level of common *J*, this flexibility is not admitted and as a consequence the m.D.–.F. single-manifold and H.–F. calculations are not comparable. This is confirmed by the fact that the single-manifold m.D.–F.–a.l. $(5p^5\,5d\,^1P)$ $6s\,^2P_{\frac{1}{2},\frac{3}{2}}$ energies are more in line with the average of configuration than the separately optimized H.–F. calculations (table 1) of Connerade & Mansfield (1978).

Downloaded from rsta.royalsocietypublishing.org

PHILOSOPHICAL TRANSACTIONS OF THE ROYAL SOCIETY A MATHEMATICAL, PHYSICAL & ENGINEERING SCIENCES

TABLE 2*a*. MIXING COEFFICIENTS IN *LS*-COUPLED BASIS FOR THE SINGLE-MANIFOLD m.D.–F.–a.l. $(5p^5\,5d)6s$ $J = \frac{1}{2}$ LEVELS OF Ba II

	level			
LS state	1	2	3	4
$(^1P)^2P_{\frac{1}{2}}$	−0.0717	0.2277	0.1476	−0.9598
	0.0147	*−0.0008*	*0.1284*	*−0.9916*
$(^3P)^2P_{\frac{1}{2}}$	0.2008	−0.8842	0.3879	−0.1651
	0.1372	*−0.9663*	*−0.2165*	*−0.0252*
$^4P_{\frac{1}{2}}$	0.9724	0.1630	−0.1567	−0.0581
	0.9868	*0.1145*	*0.1108*	*0.0289*
$^4D_{\frac{1}{2}}$	−0.0986	−0.3737	−0.8962	−0.2194
	0.0848	*0.2307*	*−0.9614*	*−0.1235*

The numbers in italics are the Hartree–Fock average of configuration plus full intermediate coupling values supplied by J. P. Connerade & M. W. D. Mansfield (1978, private communication).

TABLE 2*b*. MIXING COEFFICIENTS IN *LS*-COUPLED BASIS FOR THE SINGLE-MANIFOLD m.D.–F.–a.l. $(5p^5\,5d)6s$ $J = \frac{3}{2}$ LEVELS OF Ba II

	level						
LS state	1	2	3	4	5	6	7
$(^1P)^2P_{\frac{3}{2}}$	−0.0775	−0.2366	−0.0928	−0.1240	0.0386	0.2062	−0.9328
	−0.0287	*0.0337*	*0.0010*	*0.0877*	*−0.0799*	*−0.0793*	*−0.9888*
$(^3P)^2P_{\frac{3}{2}}$	0.1448	0.7779	0.3395	−0.1728	0.1080	−0.3605	−0.2953
	−0.1636	*0.9070*	*−0.1305*	*−0.0786*	*0.1122*	*−0.3357*	*0.0464*
$(^1D)^2D_{\frac{3}{2}}$	0.0515	−0.0524	−0.5886	0.0490	0.6575	−0.4619	−0 0138
	−0.0423	*−0.1663*	*0.4813*	*0.2940*	*0.6623*	*−0.4623*	*0.0056*
$(^3D)^2D_{\frac{3}{2}}$	0.0745	0.3167	−0.1515	−0.3434	0.4307	0.7374	0.1550
	−0.0689	*0.2406*	*0.2052*	*−0.1131*	*0.5058*	*0.7848*	*−0.1035*
$^4P_{\frac{3}{2}}$	−0.9580	0.0681	0.0692	−0.2245	0.0955	−0.0928	0.0687
	−0.9653	*−0.1143*	*0.0456*	*0.1572*	*−0.1494*	*0.0633*	*0.0451*
$^4D_{\frac{3}{2}}$	0.2166	−0.3839	0.1999	−0.8321	0.0253	−0.2429	0.1174
	−0.1844	*−0.2575*	*−0.2686*	*−0.8149*	*0.3340*	*−0.2110*	*−0.0860*
$^4F_{\frac{3}{2}}$	−0.0122	0.2896	−0.6797	−0.3029	−0.5995	−0.0535	−0.0012
	−0.0096	*−0.1067*	*−0.7969*	*0.4451*	*0.3907*	*0.0525*	*−0.0005*

The numbers in italics are the Hartree–Fock average of configuration plus full intermediate coupling values supplied by J. P. Connerade & M. W. D. Mansfield (1978, private communication).

TABLE 2*c*. MIXING COEFFICIENTS IN *LS*-COUPLED BASIS FOR THE m.D.–F.–a.l. $5d^2\,5p^5$ $J = \frac{1}{2}$ LEVELS OF Ba II

	level						
LS state	1	2	3	4	5	6	7
$(^3P)^2S_{\frac{1}{2}}$	−0.0102	−0.2889	−0.2314	0.2578	−0.8832	0.1053	0.0724
	−0.0076	*0.2517*	*0.1403*	*0.1574*	*−0.9389*	*−0.0877*	*0.0538*
$(^1S)^2P_{\frac{1}{2}}$	−0.0489	−0.1231	0.1530	−0.1791	0.0755	0.5039	0.8169
	0.0213	*−0.0713*	*0.1936*	*0.0367*	*−0.0379*	*0.8595*	*0.4642*
$(^1D)^2P_{\frac{1}{2}}$	−0.0791	−0.3746	0.7625	0.2137	−0.0576	−0.4544	0.1284
	0.0655	*−0.2483*	*0.8095*	*−0.2014*	*0.0723*	*−0.3640*	*0.3171*
$(^3P)^2P_{\frac{1}{2}}$	0.0457	0.2073	−0.4000	−0.0262	−0.0113	−0.7081	0.5410
	−0.0585	*0.1702*	*−0.4295*	*−0.0588*	*0.0494*	*−0.3255*	*0.8193*
$(^3P)^4P_{\frac{1}{2}}$	−0.0655	−0.8243	−0.4134	0.0186	0.3737	−0.0549	−0.0474
	0.0567	*−0.9040*	*−0.2993*	*−0.0532*	*−0.2910*	*−0.0378*	*0.0337*
$(^3P)^4D_{\frac{1}{2}}$	0.3176	0.1255	−0.0632	0.8800	0.2572	0.1521	0.1255
	0.3473	*−0.0943*	*0.0685*	*0.9067*	*0.1499*	*−0.1132*	*0.0913*
$(^3F)^4D_{\frac{1}{2}}$	0.9402	−0.1511	0.0817	−0.2834	−0.0707	−0.0312	−0.0171
	0.9316	*0.1220*	*−0.0945*	*−0.3238*	*−0.0470*	*0.0293*	*−0.0171*

The numbers in italics are the Hartree–Fock average of configuration plus full intermediate coupling values supplied by J. P. Connerade & M. W. D. Mansfield (1978, private communication).

Downloaded from rsta.royalsocietypublishing.org

TABLE 2*d*. MIXING COEFFICIENTS IN *LS*-COUPLED BASIS FOR THE SINGLE MANIFOLD m.D.–F.–a.l. $5d^2\,5p^5$ $J = \frac{3}{2}$ LEVELS OF Ba II

LS state	level 1	2	3	4	5	6	7	8	9	10	11
$(^1S)^2P_{\frac{3}{2}}$	−0.0440	−0.1268	0.0147	0.1206	−0.0157	−0.2731	0.0911	0.0243	−0.0915	−0.9217	0.1600
	0.0271	*0.1217*	*−0.0741*	*0.1981*	*−0.3678*	*−0.1249*	*−0.0691*	*0.2366*	*−0.8136*	*0.2570*	*0.0074*
$(^1D)^2P_{\frac{3}{2}}$	−0.0501	−0.3440	−0.2210	0.3936	−0.1000	−0.2274	−0.1317	−0.1815	0.7418	0.0582	−0.0986
	0.0441	*0.2341*	*−0.2963*	*0.4421*	*−0.3604*	*−0.2143*	*−0.1646*	*0.0626*	*0.5284*	*0.4066*	*0.0930*
$(^3P)^2P_{\frac{3}{2}}$	0.0444	0.2648	0.1110	−0.3336	0.0667	0.5356	0.2785	−0.3290	0.5055	−0.2627	0.0517
	−0.0483	*−0.1848*	*0.1237*	*−0.2621*	*0.3429*	*0.1419*	*−0.0333*	*−0.0218*	*−0.0131*	*0.8579*	*0.0629*
$(^1D)^2D_{\frac{3}{2}}$	0.0348	−0.3977	−0.4812	0.0529	−0.1154	0.4842	0.2029	0.1018	−0.2150	−0.1308	−0.4937
	0.0093	*0.2102*	*−0.5479*	*0.3111*	*0.5346*	*0.2239*	*−0.1006*	*−0.0970*	*−0.1447*	*−0.0081*	*−0.4270*
$(^3P)^2D_{\frac{3}{2}}$	−0.0713	0.0722	0.0188	0.2047	0.6955	0.1260	−0.4612	−0.3590	−0.1385	−0.1170	−0.2709
	−0.0633	*0.0708*	*−0.0776*	*−0.1186*	*0.1703*	*−0.6135*	*0.6259*	*0.2823*	*0.0534*	*0.0738*	*−0.2928*
$(^3F)^2D_{\frac{3}{2}}$	0.0264	0.2269	0.2505	−0.2496	−0.0580	−0.3850	0.0937	0.1148	0.1346	−0.0843	−0.7899
	0.0338	*−0.1273*	*0.3433*	*−0.0185*	*−0.2991*	*0.0337*	*−0.2111*	*−0.0660*	*0.0948*	*0.0866*	*−0.8417*
$^4S_{\frac{3}{2}}$	−0.0179	−0.1359	0.1917	−0.1832	−0.0036	0.2945	−0.5684	0.6444	0.2511	−0.1491	0.0207
	0.0123	*0.1576*	*0.1066*	*−0.1394*	*0.2063*	*0.0533*	*−0.4128*	*0.8376*	*0.1237*	*−0.1069*	*−0.0072*
$(^3P)^4P_{\frac{3}{2}}$	0.1403	0.6900	−0.5751	0.2358	0.0486	−0.0273	−0.0346	0.3090	0.1096	−0.0748	0.0232
	0.1201	*0.8697*	*0.3197*	*−0.2118*	*0.0749*	*−0.0492*	*−0.0351*	*−0.2629*	*−0.0298*	*0.0522*	*0.0112*
$(^3P)^4D_{\frac{3}{2}}$	0.4565	−0.2266	0.1085	0.0837	0.6025	−0.0798	0.4436	0.3517	0.1377	0.0872	0.0706
	0.3901	*0.0998*	*0.0976*	*0.1668*	*−0.1482*	*0.6141*	*0.5651*	*0.2633*	*0.0828*	*0.0702*	*−0.0319*
$(^3F)^4D_{\frac{3}{2}}$	0.8446	−0.0644	−0.0907	−0.1918	−0.2100	−0.0740	−0.3300	−0.2655	−0.0661	−0.0637	0.0109
	0.8893	*−0.1918*	*0.0413*	*0.0453*	*0.1842*	*−0.3106*	*−0.1674*	*−0.0786*	*−0.0412*	*−0.0179*	*0.0443*
$(^3F)^4F_{\frac{3}{2}}$	−0.2118	−0.1747	−0.5065	−0.6923	0.2746	−0.2983	−0.0641	−0.0294	0.0621	0.0271	0.1219
	0.1792	*0.0530*	*−0.5852*	*−0.7009*	*−0.3302*	*0.1091*	*−0.0396*	*−0.0042*	*0.0339*	*0.0110*	*−0.0873*

The numbers in italics are the Hartree–Fock average of configuration plus full intermediate coupling values supplied by J. P. Connerade & M. W. D. Mansfield (1978, private communication).

Downloaded from rsta.royalsocietypublishing.org

Table 3*a*. Energy levels and mixing coefficients for the triple-manifold m.D.–F.–a.l. $J=\frac{1}{2}$ Ba II calculation

LS state	level 1	2	3	4	5	6	7	8	9	10	11	12
$5p^5\,6s^2\,{}^2P_{\frac{1}{2}}$	0.0040	0.0153	0.1235	−0.0077	0.0162	0.0639	−0.0801	−0.8902	0.0727	−0.3698	0.1050	−0.1676
$5p^5\,5d\,6s\,({}^1P)\,{}^2P_{\frac{1}{2}}$	−0.0017	−0.0641	−0.1918	0.0393	0.0933	0.1316	0.0283	−0.0015	0.0100	−0.2301	−0.9228	−0.1615
$({}^3P)\,{}^2P_{\frac{1}{2}}$	0.0219	0.1513	0.8388	−0.1737	−0.2930	0.3195	−0.0574	0.1007	−0.0231	0.0644	−0.1872	−0.0426
${}^4P_{\frac{1}{2}}$	0.5147	0.8139	−0.0983	0.1998	−0.0560	−0.1279	0.0068	−0.0076	−0.0300	−0.0204	−0.0459	−0.0088
${}^4D_{\frac{1}{2}}$	−0.1926	0.0096	0.2378	−0.1041	−0.1653	−0.9111	0.0049	−0.0201	0.0111	−0.0678	−0.1768	−0.0389
$5p^5\,5d^2\,({}^3P)\,{}^2S_{\frac{1}{2}}$	−0.0159	−0.0432	0.0211	0.3115	−0.2077	0.0181	0.2549	0.0159	0.8812	0.1025	−0.0029	−0.0682
$({}^1S)\,{}^2P_{\frac{1}{2}}$	0.0395	−0.0416	0.0257	0.1116	0.1798	−0.0570	−0.1864	−0.0874	−0.0680	0.5793	−0.0069	−0.7519
$({}^1D)\,{}^2P_{\frac{1}{2}}$	0.0637	−0.0171	0.3636	0.2312	0.7158	−0.0685	0.2465	0.2345	0.0364	−0.3708	0.1244	−0.1510
$({}^3P)\,{}^2P_{\frac{1}{2}}$	−0.0357	0.0146	−0.1727	0.1414	−0.3987	0.0631	−0.0170	0.3329	−0.0238	−0.5361	0.2310	−0.5773
$({}^3P)\,{}^4P_{\frac{1}{2}}$	−0.0490	−0.1998	0.0988	0.8335	−0.3222	−0.0042	0.0187	−0.0197	−0.3782	−0.0595	−0.0008	0.0449
$({}^3P)\,{}^4D_{\frac{1}{2}}$	−0.2591	0.1764	−0.0526	−0.1166	−0.0820	0.0689	0.8664	−0.1439	−0.2502	0.1611	0.0004	−0.1186
$({}^3F)\,{}^4D_{\frac{1}{2}}$	−0.7879	0.4849	−0.0487	0.1620	0.1317	0.1141	−0.2787	0.0460	0.0661	−0.0244	0.0097	0.0159
energy/cm^{-1}†	126 098	126 519	132 971	140 119	143 540	150 255	156 776	159 457	161 561	177 044	186 921	189 266

† Relative to single manifold m.D.–F. $5p^6\,6s\,{}^2S_{\frac{1}{2}}$ state. *LS* states based on the configuration $5d^2\,5p^5$ and not $5p^5\,5d^2$ were used, so as to be consistent with the eigenvectors of Connerade & Mansfield (1978, private communication), table 2.

Downloaded from rsta.royalsocietypublishing.org

Table 3*b*. Energy levels and mixing coefficients for the triple-manifold m.D.–F.–al. $J = \frac{3}{2}$ Ba ii calculation

LS state	level 1	2	3	4	5	6	7	8	9
$5p^5\,6s^2\,{}^2P_{\frac{3}{2}}$	0.0037	−0.0492	−0.2546	0.1415	0.0212	−0.4930	−0.6406	−0.0295	−0.3109
$5p^5\,5d\,6s\,({}^1P){}^2P_{\frac{3}{2}}$	−0.0147	−0.1355	−0.1467	0.0747	0.0317	−0.2526	0.1263	−0.2574	0.2222
$({}^3P){}^2P_{\frac{3}{2}}$	−0.0076	0.0413	0.4070	0.0458	0.0789	0.0587	−0.2896	0.0531	0.4234
$({}^1D){}^2D_{\frac{3}{2}}$	−0.0030	−0.0290	−0.2806	0.2156	−0.4432	−0.0481	0.1302	−0.3872	0.0752
$({}^3D){}^2D_{\frac{3}{2}}$	0.0155	0.1958	0.2968	0.0479	−0.2168	0.3224	−0.3121	0.1493	0.0519
${}^4P_{\frac{3}{2}}$	0.1688	−0.8895	0.0731	0.1582	0.1955	0.1555	−0.0097	−0.0196	0.0853
${}^4D_{\frac{3}{2}}$	−0.1987	0.1642	−0.1142	−0.1743	0.2119	−0.2915	0.2025	−0.1594	0.4698
${}^4F_{\frac{3}{2}}$	0.0194	−0.0114	0.0166	0.3743	−0.5731	0.1479	−0.0901	−0.2008	0.2124
$5p^5\,5d^2\,({}^1S){}^2P_{\frac{3}{2}}$	0.0381	0.0315	−0.0590	0.0825	0.0521	−0.0001	−0.1026	0.1276	0.1832
$({}^1D){}^2P_{\frac{3}{2}}$	0.0389	−0.0116	−0.3501	0.0359	−0.0074	0.1000	0.0566	0.3228	0.4072
$({}^3P){}^2P_{\frac{3}{2}}$	−0.0355	0.0045	0.2776	−0.1209	−0.0386	0.1256	0.3524	−0.3006	−0.2941
$({}^1D){}^2D_{\frac{3}{2}}$	−0.0391	−0.0238	−0.4489	−0.2030	−0.0662	0.3935	−0.0277	0.1426	−0.1253
$({}^3P){}^2D_{\frac{3}{2}}$	0.0703	−0.0053	−0.0065	0.0037	−0.0696	−0.0871	0.1342	0.1608	−0.0436
$({}^3F){}^2D_{\frac{3}{2}}$	−0.0235	0.0121	0.3104	0.0648	0.1005	−0.1742	−0.0998	−0.2600	0.1105
${}^4S_{\frac{3}{2}}$	0.0074	0.0577	0.0007	0.1595	0.1434	0.0865	0.0511	−0.1659	−0.2098
$({}^3P){}^4P_{\frac{3}{2}}$	−0.0830	−0.2966	0.1559	−0.6208	−0.5103	−0.2882	−0.0294	0.1778	0.0458
$({}^3P){}^4D_{\frac{3}{2}}$	−0.4503	−0.0429	−0.0607	0.1836	0.1019	0.1125	−0.0088	0.1218	0.0599
$({}^3F){}^4D_{\frac{3}{2}}$	−0.8204	−0.1552	0.0026	−0.0436	0.0019	0.1389	−0.1421	−0.1235	−0.0633
$({}^3F){}^4F_{\frac{3}{2}}$	0.1928	0.0299	−0.1832	−0.4620	0.1496	0.3337	−0.3686	−0.5272	0.1546
energy/cm^{-1}†	126 606	128 147	132 560	137 648	138 305	139 444	142 967	143 716	148 934

† Relative to single manifold m.D.–F. $5p^6\,6s\,{}^2S_{\frac{1}{2}}$ state.

Downloaded from rsta.royalsocietypublishing.org

	level									
LS state	10	11	12	13	14	15	16	17	18	19
$5p^5\,6s^2\,{}^2P_{\frac{3}{2}}$	0.0480	0.1869	0.1064	0.0673	0.0503	−0.2593	−0.1913	−0.0280	−0.0350	−0.0011
$5p^5\,5d\,6s\,(^1P)\,{}^2P_{\frac{3}{2}}$	−0.0115	−0.0559	0.0089	0.0027	−0.1037	−0.2337	0.5066	−0.6475	0.1105	0.0332
$(^3P)\,{}^2P_{\frac{3}{2}}$	−0.0010	0.1624	0.1817	−0.0549	−0.1008	−0.4305	0.3658	0.3823	−0.0656	−0.1125
$(^1D)\,{}^2D_{\frac{3}{2}}$	0.1165	−0.3988	0.4559	0.0116	−0.0163	−0.0209	0.0063	0.3338	−0.0816	−0.0574
$(^3D)\,{}^2D_{\frac{3}{2}}$	0.1029	−0.0950	0.5031	−0.0132	0.0632	0.1025	−0.1916	−0.4988	0.1311	0.0872
${}^4P_{\frac{3}{2}}$	0.0255	0.0908	0.1786	0.0122	0.0811	0.1006	−0.1484	−0.0017	0.0051	0.0101
${}^4D_{\frac{3}{2}}$	0.0234	0.4549	0.3368	0.0428	0.1134	0.2272	−0.2924	0.0016	0.0019	0.0194
${}^4F_{\frac{3}{2}}$	−0.0580	0.4734	−0.4110	0.0076	0.0376	0.0892	−0.0792	−0.0522	0.0103	0.0189
$5p^5\,5d^2\,(^1S)\,{}^2P_{\frac{3}{2}}$	−0.0121	−0.1310	−0.0629	0.0937	0.0331	0.1623	0.0112	−0.1960	−0.8823	−0.2229
$(^1D)\,{}^2P_{\frac{3}{2}}$	−0.1269	−0.2163	−0.1400	−0.2222	−0.1072	−0.4755	−0.4490	−0.0603	0.0598	0.1143
$(^3P)\,{}^2P_{\frac{3}{2}}$	0.0440	0.1670	0.0532	0.2079	0.0957	−0.5792	−0.2918	−0.1342	−0.2471	−0.0631
$(^1D)\,{}^2D_{\frac{3}{2}}$	−0.1222	0.3222	0.2231	0.2083	−0.0686	−0.0761	0.2940	0.0618	−0.1810	0.4624
$(^3P)\,{}^2D_{\frac{3}{2}}$	0.6858	0.1090	−0.0395	−0.4777	0.3454	−0.0704	0.1253	0.0123	−0.1408	0.2546
$(^3F)\,{}^2D_{\frac{3}{2}}$	−0.0519	−0.2454	−0.1480	0.1004	−0.1208	0.0691	−0.1242	0.0606	−0.1582	0.7811
${}^4S_{\frac{3}{2}}$	0.0018	0.2027	0.1306	−0.5346	−0.6993	0.0795	−0.0864	−0.0443	−0.1395	−0.0288
$(^3P)\,{}^4P_{\frac{3}{2}}$	0.0433	0.0033	−0.0191	−0.0228	−0.3243	0.0432	−0.0385	−0.0245	−0.0687	−0.0269
$(^3P)\,{}^4D_{\frac{3}{2}}$	0.5919	−0.0381	−0.1267	0.4480	−0.3639	−0.0029	−0.0574	0.0054	0.0912	−0.0624
$(^3F)\,{}^4D_{\frac{3}{2}}$	−0.2112	−0.1011	−0.0470	−0.3402	0.2534	−0.0154	0.0322	−0.0192	−0.0593	−0.0151
$(^3F)\,{}^4F_{\frac{3}{2}}$	0.2567	−0.0877	−0.2122	−0.0663	0.0174	0.0179	−0.0681	−0.0165	0.0395	−0.1154
energy/cm^{-1}†	150 629	153 421	153 462	158 857	161 506	163 998	169 334	181 576	190 757	193 683

† Relative to single manifold m.D.–F. $5p^6\,6s\,{}^2S_{\frac{1}{2}}$ state.

Downloaded from rsta.royalsocietypublishing.org

M.c. H.–F. calculations have been performed by Hansen (1975*b*) on the same two levels. In addition to the separate level optimization the $5p^5\,6s^2$ and $5p^5\,5d\,6s$ configurations were allowed different 6s and 5d orbitals from the $5p^5\,5d^2$ configuration and no comparison between these and the m.D.–F. triple-manifold results is attempted.

4. THE USE OF INTENSITY RATIOS AND ENERGY SEPARATIONS IN THE INTERPRETATION OF THE ELECTRON-IMPACT IONIZATION SPECTRUM OF Ba I

The electron-impact experiment of Mehlhorn *et al.* (1977) produces Ba II states by ionization of a 5p shell electron. Decay to the Ba III ground state follows, accompanied by ejection of an Auger electron whose kinetic energy is equal to the energy of the particular Ba II state relative to the Ba III ground state. The intensity of signal is proportional to the probability of production of the particular Ba II state, and so as to make use of this information as well, a simple model for the electron-impact ionization process is proposed. The ground Ba I state is labelled α and has $J = 0$, while that of the ionized Ba II state is called β. The state β plus ejected 5p electron is called γ and has $J = 1$; it can be constructed from c.s.fs used for Ba II with $J = \frac{1}{2}, \frac{3}{2}, \frac{5}{2}$ or $\frac{7}{2}$ by coupling an outgoing continuum ϵs, $\epsilon\bar{d}$ or ϵd electron†

Rose *et al.* (1978) have performed such an m.D.–F. – a.l. calculation for the Ba I ground state and found its composition to be

$$\Psi_\alpha = 0.9780[6s^2\,5\bar{p}^2\,5p^4] - 0.1337[5\bar{d}_0^2\,5\bar{p}^2\,5p^4]_0 - 0.1600[5d_0^2\,5\bar{p}^2\,5p^4]_0. \tag{2}$$

TABLE 4. ORBITAL RADII FOR Ba I AND Ba II MULTIPLE MANIFOLD CALCULATIONS

	$\langle r\rangle/a_0$		
		Ba II	
orbital	Ba I: double manifold a.l. $J = 0$	triple manifold a.l. $J = \frac{1}{2}$	triple manifold a.l. $J = \frac{3}{2}$
$5\bar{p}$	1.8832	1.8462	1.8446
5p	1.9622	1.9141	1.9153
$5\bar{d}$	4.7459	3 0582	3.0888
5d	4.9081	3.2662	3.2043
6s	5.0545	4.2802	4.3055

Table 4 shows the radii of each orbital for the multiple manifold calculations on Ba I and Ba II. Although the $5\bar{p}$ and 5p orbitals are similar for each calculation the $5\bar{d}$, 5d and 6s are contracted in the ionic state. For simplicity we make the approximation that the mixing coefficients taken from separate calculations correspond to some common set of orbitals, ignoring the effects of orbital relaxation.

Mott & Massey (1965, § 9.21) derive an approximate expression for the ionization cross-section from electron-impact at high energy (greater than 1 keV, but not such that kinematic relativistic effects are important, a criterion which is satisfied for 2 keV electrons). They show that for fixed initial impact energy the ionization cross section from ground state α to ionic state β involving a continuum electron of angular character κ is given by

$$Q^i_{\beta\leftarrow\alpha}(\kappa) \propto \int |d_{z\alpha\gamma}(\epsilon\kappa)|^2\,\mathrm{d}\epsilon, \tag{3}$$

---

† The symbols $\bar{l}$ and l conventionally distinguish between Dirac orbitals having respectively $j = l-\frac{1}{2}$ and $j = l+\frac{1}{2}$.

PHILOSOPHICAL TRANSACTIONS OF THE ROYAL SOCIETY A MATHEMATICAL, PHYSICAL & ENGINEERING SCIENCES

PHILOSOPHICAL TRANSACTIONS OF THE ROYAL SOCIETY A MATHEMATICAL, PHYSICAL & ENGINEERING SCIENCES

Downloaded from rsta.royalsocietypublishing.org

where $d_{z\alpha\gamma}(\epsilon\kappa)$ is the dipole matrix element for transition from ground state α to ionizing state γ involving continuum electron $\epsilon\kappa$ and the integral is over all possible continuum states of fixed κ, the sum over M_γ values being incorporated in $|d_{z\alpha\gamma}(\epsilon\kappa)|^2$. With the assumptions that the c.s.f. mixing coefficients for the ionization state γ can be taken as those of the corresponding Ba II ion, and that the radial factors involved in $|d_{z\alpha\gamma}(\epsilon\kappa)|^2$ are independent of the Ba II state β, then equation (3) can be written as (see the appendix)

$$Q^{i}_{\beta\leftarrow\alpha} = \text{const.}\,(D^{\mathrm{e}\kappa}_{\alpha\beta})^2, \tag{4}$$

where

$$D^{\mathrm{e}\kappa}_{\alpha\beta} = \sum_{\mathrm{r,s}} c_{\mathrm{r}\alpha}\, c_{\mathrm{s}\beta}\, d^{(1)}_{\mathrm{e}\kappa}\,(\mathrm{r,s}) \tag{5}$$

and $\mathrm{e} \equiv \bar{\mathrm{p}}$ if $J = \frac{1}{2}$ and p if $J = \frac{3}{2}$. In this approximation the ionization cross section depends only on configuration interaction in the initial state (i.s.c.i.) and in the final ionic state (f.i.s.c.i.) together with the angular factor $d^{(1)}_{ab}(\mathrm{r,s})$ (table 5), which physically accounts for the degeneracy of the ionized subshell ($5\bar{\mathrm{p}}$ or 5p) and only allows nonvanishing transition matrix elements between c.s.fs with appropriate angular structure. This approximation is similar in form and physical content to those derived by Martin & Shirley (1976) for the interpretation of photoemission satellite spectra in the non-relativistic approximation.

Equation (2) shows that the ground state of Ba I is predominantly $[6\mathrm{s}^2\,5\bar{\mathrm{p}}^2\,5\mathrm{p}^4]_0$ and so it proves convenient to split up the sum $D^{\mathrm{e}\kappa}_{\alpha\beta}$ as follows

$$D^{\mathrm{e}\kappa}_{\alpha\beta} = E^{\mathrm{e}\kappa}_{\alpha\beta} + F^{\mathrm{e}\kappa}_{\alpha\beta}, \tag{6}$$

where

$$E^{\mathrm{e}\kappa}_{\alpha\beta} = \sum_{\mathrm{s}} c_{1\alpha}\, c_{\mathrm{s}\beta}\, d^{(1)}_{e\kappa}(1,\mathrm{s}) \tag{7}$$

and

$$F^{\mathrm{e}\kappa}_{\alpha\beta} = \sum_{\mathrm{r}=2,3}\, \sum_{\mathrm{s}} c_{\mathrm{r}\alpha}\, c_{\mathrm{s}\beta}\, d^{(1)}_{e\kappa}(\mathrm{r,s}). \tag{8}$$

For $J_\beta = \frac{1}{2}$, $(E^{\mathrm{e}\kappa}_{\alpha\beta})^2$ depends on the $[6\mathrm{s}^2\,5\bar{\mathrm{p}}\,5\mathrm{p}^4]_{\frac{1}{2}}$ character and for $J_\beta = \frac{3}{2}$ on the $[6\mathrm{s}^2\,5\bar{\mathrm{p}}^2\,5\mathrm{p}^3]_{\frac{3}{2}}$ character of the ionic state (which in *LS*-coupling is equivalent to $5\mathrm{p}^5\,6\mathrm{s}^2\,{}^2\mathrm{P}_{\frac{1}{2}}$ or ${}^2\mathrm{P}_{\frac{3}{2}}$ character) weighted in each case by $2J_\beta + 1$ and is the contribution from f.i.s.c.i. alone. The second term in (6) results from a combination of configuration interaction in the ground and ionic states, the interacting c.s.fs that contribute being $[5\bar{\mathrm{d}}^2_0\,5\bar{\mathrm{p}}^2\,5\mathrm{p}^4]_0$ and $[5\mathrm{d}^2\,5\bar{\mathrm{p}}^2\,5\mathrm{p}^4]_0$ in the ground state α and $[[5\bar{\mathrm{d}}^2_0\,5\bar{\mathrm{p}}\,5\mathrm{p}^4]_{\frac{1}{2}}\,\epsilon\kappa]_1$, $[[5\bar{\mathrm{d}}^2_0\,5\bar{\mathrm{p}}^2\,5\mathrm{p}^3]_{\frac{3}{2}}\,\epsilon\kappa]_1$, $[[5\mathrm{d}^2_0\,5\bar{\mathrm{p}}\,5\mathrm{p}^4]_{\frac{1}{2}}\,\epsilon\kappa]_1$ and $[[5\mathrm{d}^2_0\,5\bar{\mathrm{p}}^2\,5\mathrm{p}^3]_{\frac{3}{2}}\,\epsilon\kappa]_1$ in the ionizing state γ (table 5). The values of $(D^{\mathrm{e}\kappa}_{\alpha\beta})^2$ and $(E^{\mathrm{e}\kappa}_{\alpha\beta})^2$ are shown for the different levels β in table 6, and are very similar except for several levels high in energy for which $(D^{\mathrm{e}\kappa}_{\alpha\beta})^2$ is significantly greater than $(E^{\mathrm{e}\kappa}_{\alpha\beta})^2$, although this does not affect identification of the experimental levels. This shows that inclusion of such configuration interaction in $(D^{\mathrm{e}\kappa}_{\alpha\beta})^2$ produces a correction to the simplest approximation $(E^{\mathrm{e}\kappa}_{\alpha\beta})^2$, which is unimportant for our purposes.

Figure 2 shows the assignment of each of the six prominent peaks in the experimental spectrum of Mehlhorn *et al.* (1977) (figure 2(i)) on the basis of energy and intensity (figure 2(ii)). The major feature of the experimental electron-impact spectrum of Ba I which differs from the lighter alkaline earths is that instead of two strong peaks corresponding to $5\mathrm{p}^5\,6\mathrm{s}^2\,{}^2\mathrm{P}_{\frac{1}{2}}$ and ${}^2\mathrm{P}_{\frac{3}{2}}$, three major peaks are seen. Our identifications show that the most intense peak corresponds to a Ba II state ($J = \frac{1}{2}$ level 8) which is predominantly $5\mathrm{p}^5\,6\mathrm{s}^2\,{}^2\mathrm{P}_{\frac{1}{2}}$ (79 %). However, the two other

PHILOSOPHICAL TRANSACTIONS OF THE ROYAL SOCIETY A MATHEMATICAL, PHYSICAL & ENGINEERING SCIENCES

PHILOSOPHICAL TRANSACTIONS OF THE ROYAL SOCIETY A MATHEMATICAL, PHYSICAL & ENGINEERING SCIENCES

Downloaded from rsta.royalsocietypublishing.org

PHILOSOPHICAL TRANSACTIONS OF THE ROYAL SOCIETY A MATHEMATICAL, PHYSICAL & ENGINEERING SCIENCES

Table 5. Non-zero values of the coefficient $d^{(1)}_{ab}(\mathrm{r}, \mathrm{s})$

a	b	r	s	$d^{(1)}_{ab}(\mathrm{r},\mathrm{s})$
$5\bar{p}$	$n\kappa$	$[6s^2\,5\bar{p}^2\,5p^4]_0$	$[[6s^2\,5\bar{p}\,5p^4]_{\frac{1}{2}}\,n\kappa]_1$	$\sqrt{2}$
$5\bar{p}$	$n\kappa$	$[5\bar{d}^2_0\,5\bar{p}^2\,5p^4]_0$	$[[5\bar{d}^2_0\,5\bar{p}\,5p^4]_{\frac{1}{2}}\,n\kappa]_1$	$\sqrt{2}$
$5\bar{p}$	$n\kappa$	$[5d^2_0\,5\bar{p}^2\,5p^4]_0$	$[[5d^2_0\,5\bar{p}\,5p^4]_{\frac{1}{2}}\,n\kappa]_1$	$\sqrt{2}$
$5p$	$n\kappa$	$[6s^2\,5\bar{p}^2\,5p^4]_0$	$[[6s^2\,5\bar{p}^2\,5p^3]_{\frac{3}{2}}\,n\kappa]_1$	2
$5p$	$n\kappa$	$[5\bar{d}^2_0\,5\bar{p}^2\,5p^4]_0$	$[[5\bar{d}^2_0\,5\bar{p}^2\,5p^3]_{\frac{3}{2}}\,n\kappa]_1$	2
$5p$	$n\kappa$	$[5d^2_0\,5\bar{p}^2\,5p^4]_0$	$[[5d^2\,5\bar{p}^2\,5p^3]_{\frac{3}{2}}\,n\kappa]_1$	2

Table 6. The triple-manifold AL $J = \frac{1}{2}$ and $J = \frac{3}{2}$ energy levels and $(D^{e\kappa}_{\alpha\beta})^2$ and $(E^{e\kappa}_{\alpha\beta})^2$ values for each level (see text)

level β				
J	level	energy/cm⁻¹†	$(D^{e\kappa}_{\alpha\beta})^2$	$(E^{e\kappa}_{\alpha\beta})^2$
$\frac{1}{2}$	1	126 098	0.0015	$< 10^{-4}$
$\frac{1}{2}$	2	126 519	0.0003	0.0004
$\frac{3}{2}$	1	126 606	0.0003	0.0001
$\frac{3}{2}$	2	128 147	0.0091	0.0093
$\frac{3}{2}$	3	132 560	0.3213	0.2480
$\frac{1}{2}$	3	132 971	0.0355	0.0292
$\frac{3}{2}$	4	137 648	0.1043	0.0766
$\frac{3}{2}$	5	138 305	0.0033	0.0016
$\frac{3}{2}$	6	139 444	1.0527	0.9297
$\frac{1}{2}$	4	140 119	0.0001	0.0001
$\frac{3}{2}$	7	142 967	1.9597	1.5700
$\frac{1}{2}$	5	143 540	0.0053	0.0007
$\frac{3}{2}$	8	143 716	0.0006	0.0033
$\frac{3}{2}$	9	148 934	0.2918	0.3698
$\frac{1}{2}$	6	150 255	0.0058	0.0078
$\frac{3}{2}$	10	150 629	0.0089	0.0088
$\frac{3}{2}$	11	153 421	0.1061	0.1337
$\frac{3}{2}$	12	153 462	0.0415	0.0433
$\frac{1}{2}$	7	156 766	0.0168	0.0123
$\frac{3}{2}$	13	158 857	0.0056	0.0173
$\frac{1}{2}$	8	159 457	1.8090	1.5161
$\frac{3}{2}$	14	161 506	0.0053	0.0097
$\frac{1}{2}$	9	161 561	0.0107	0.0101
$\frac{3}{2}$	15	163 998	0.0477	0.2573
$\frac{3}{2}$	16	169 334	0.0413	0.1401
$\frac{1}{2}$	10	177 044	0.1086	0.2616
$\frac{3}{2}$	17	184 576	$< 10^{-4}$	0.0030
$\frac{1}{2}$	11	186 921	0.0048	0.0211
$\frac{1}{2}$	12	189 266	0.0030	0.0538
$\frac{3}{2}$	18	190 757	0.0005	0.0047
$\frac{3}{2}$	19	193 683	0.0001	$< 10^{-4}$

† All energies referred to the single manifold calculation on the ground state of Ba II ($5p^6\,6s$).

peaks are due to two different Ba II states ($J = \frac{3}{2}$ levels 6 and 7), which have 24 % and 41 % $5p^5\,6s^2\,{}^2P_{\frac{3}{2}}$ character respectively (table 3). The fact that two levels can have significant $5p^5\,6s^2\,{}^2P_{\frac{3}{2}}$ character is solely due to the 6s–5d mixing in the Ba II levels.

5. Interpretation of the 5p photoabsorption spectrum of Ba I

The 5p photoabsorption spectrum of Ba I has been presented by Connerade *et al.* (1979), who identify 14 series converging on 12 series limits (denoted (a, b), $c, d, e, f, g, h, i, j, k$ and l). In the photoabsorption process in which a 5p electron is excited to a Rydberg state, there are several

Downloaded from rsta.royalsocietypublishing.org

PHILOSOPHICAL TRANSACTIONS OF THE ROYAL SOCIETY A MATHEMATICAL, PHYSICAL & ENGINEERING SCIENCES

complicating features which invalidate the simple predictions of intensity that we were able to make for the electron-impact spectrum.

(i) In the photoabsorption case the continuum orbital is replaced by a Rydberg orbital which is bound. As the electron is below threshold, the orbital, and thus the radial transition matrix elements involved in the photoabsorption transition probability, will be dependent on the Ba II state. This is consistent with the work of Connerade *et al.* (1979*a*) which shows that only one of the series limits, (a, b), supports both $l = 0$ and $l = 2$ series.

(ii) Interchannel coupling is known experimentally to be significant (Connerade *et al.* (1979*a*)) and can transfer intensity from one series to another.

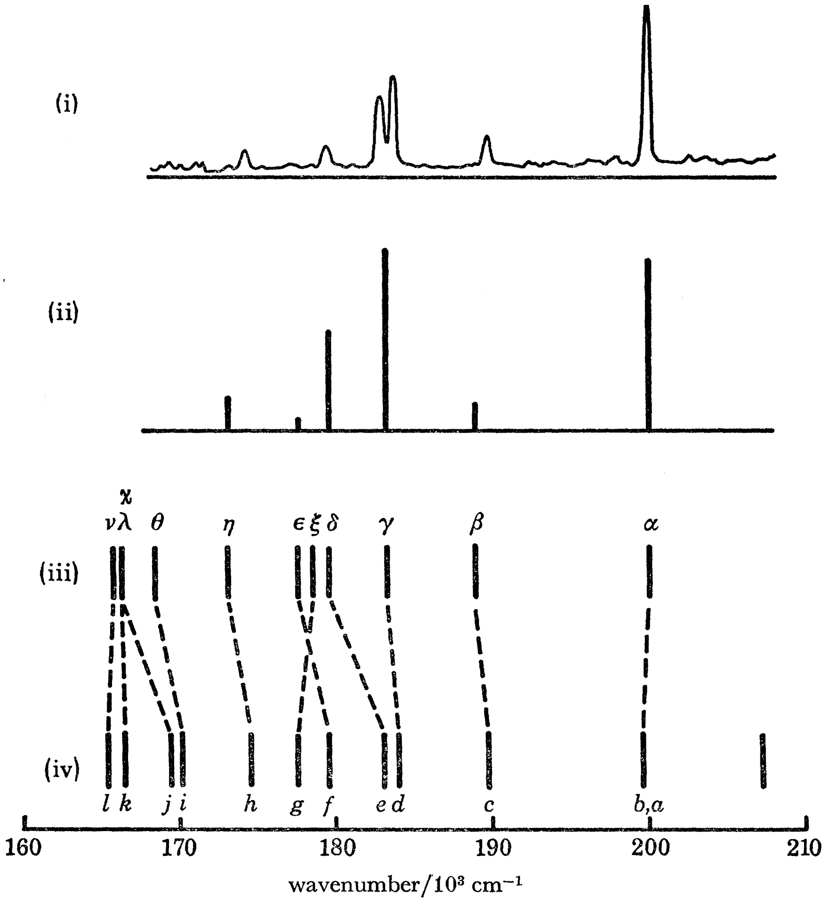

FIGURE 2. (i) Experimental Ba I 2 keV electron-impact 5p-ionization spectrum of Mehlhorn *et al.* (1977). (ii) Predicted relative intensity and position of the electron-impact ionization peaks (i) from the present triple-manifold m.D.–F.–a.l. calculations using $(D^{\text{cs}}_{\alpha\beta})^2$ (table 6). (The intensity and position of level α is taken to be that of the most prominent peak). (iii) Predicted position of Ba I 5p-photoabsorption series limits made on the basis of the correspondence between the electron-impact ionization experiment and 5p-photoabsorption experiment (figure 1). (iv) Experimental Ba I 5p-photoabsorption series limits (Connerade *et al.* 1979). The labels α–ν correspond to the following triple-manifold m.D.–F.–a.l. levels:

α $J = \frac{1}{2}$, level 8.
β $J = \frac{3}{2}$, level 9.
γ $J = \frac{3}{2}$, level 7.
δ $J = \frac{3}{2}$, level 6.
ϵ $J = \frac{3}{2}$, level 4.
η $\begin{cases} J = \frac{1}{2}, \text{ level 3.} \\ J = \frac{3}{2}, \text{ level 3.} \end{cases}$

$\left.\begin{array}{ll} \xi & J = \frac{3}{2}, \text{ level 5.} \\ \theta & J = \frac{3}{2}, \text{ level 2.} \\ \chi & J = \frac{3}{2}, \text{ level 1.} \\ \lambda & J = \frac{1}{2}, \text{ level 2.} \\ \nu & J = \frac{1}{2}, \text{ level 1.} \end{array}\right\}$ tentatively assigned

Downloaded from rsta.royalsocietypublishing.org

MATHEMATICAL, PHYSICAL & ENGINEERING SCIENCES
PHILOSOPHICAL TRANSACTIONS OF THE ROYAL SOCIETY A
MATHEMATICAL, PHYSICAL & ENGINEERING SCIENCES
PHILOSOPHICAL TRANSACTIONS OF THE ROYAL SOCIETY A

The assignments for the electron-impact ionization spectrum can be carried over to identify the limits (a, b), c, d, e, f and h in the photoabsorption spectrum (figure 2 (iii) and (iv)) on the basis of the correspondence between the two experiments suggested by Connerade *et al.* (1979*a*) (figure 1). Certain complicating features of the limits (a, b) and h remain, however.

The photoabsorption spectrum suggests that there are three series converging on two limits very close in energy denoted by (a, b) (see tables 1*a* and *b* of Connerade *et al.* (1979*a*)). We suggest that the ns and $n\bar{d}$ series converge to a limit which is assigned to $J = \frac{1}{2}$ level 8, as is the corresponding peak in the electron-impact ionization spectrum. The other (possibly ns) series limit cannot be readily identified since no other level of significant $(D^{e\kappa}_{\alpha\beta})^2$ (table 6) is close enough to $J = \frac{1}{2}$ level 8. One explanation is that this other series borrows its intensity by mixing with the first series (which is supported by the fact that only the first few members are seen) and in fact converges to another level, possibly $J = \frac{3}{2}$ level 13 which lies 600 cm^{-1} below $J = \frac{1}{2}$ level 8.

Connerade *et al.* (1979*a*) suggested that two series converge on limits close in energy which are denoted jointly by h (the electron-impact ionization experiment presumably cannot resolve the two) and the m.D.–F. calculations predict two levels which were assigned jointly to the electron-impact peak corresponding to the limit h. No prediction is made as to which series converges to which limit since the two are so close in energy.

Five series limits remain which we consider cannot be unambiguously matched with the peaks in the electron-impact ionization spectrum: g, i, j, k and l. In this low-energy region, exactly five previously unassigned levels are predicted by the m.D.–F. calculations, although each has a low value of $(D^{e\kappa}_{\alpha\beta})^2$ in table 6. Interaction between channels, which is experimentally conspicuous, may be responsible for their appearance and, as in general Hamiltonian matrix elements of the form

$$\langle[[\mu]_{j1}n\kappa]_1|\,H\,|[[\nu]_{j2}n\kappa]_1\rangle \neq 0, \tag{9}$$

where $[\mu]_{j1}$ and $[\nu]_{j2}$ are two 5p-ionized Ba II c.s.fs with $j_1, j_2 = \frac{1}{2}, \frac{3}{2}, \frac{5}{2} \ldots$, there is the possibility that these series have Ba II limits of $J > \frac{3}{2}$. However, the fact that each limit is associated with a line in Roig's (1976) list (Connerade *et al.* 1979*a*) which involves a transition from the Ba II ground state ($J = \frac{1}{2}$), suggests that the limits g, i, j, k and l have $J = \frac{1}{2}$ or $\frac{3}{2}$ and are consequently tentatively assigned in order of energy to the five remaining triple-manifold m.D.–F. $J = \frac{1}{2}$ and $\frac{3}{2}$ levels (but see Connerade *et al.* 1979*b*).

The experimental 5p-subshell spectrum of Ba I (Connerade *et al.* (1979*a*)), with the assignments of series limits from the present work is shown in figure 3.

6. Conclusions

Comparison between single configuration non-relativistic Hartree–Fock intermediate coupling calculations and single manifold m.D.–F. – a.l. results shows differences in the ordering of levels. As interaction between the configurations 5p^5 6s^2, 5p^5 5d 6s and 5p^5 5d^2 was expected to account for the prominence of more than two (formally 5p^5 6s^2 ^{2}P$_{\frac{1}{2},\frac{3}{2}}$) states in the electron-impact 5p-ionization spectrum (Mehlhorn *et al.* 1977) and more than two series in the 5p-photoabsorption spectrum of Ba I, a model of the (theoretically simpler) electron-impact ionization process is used which ignores variation in orbitals between one level and one ionization state and another but does include the effect of configuration interaction in both Ba I and Ba II states. The six most prominent peaks in the ionization experiment can then be assigned on the basis of predicted energy and intensity employing only final ionic state configuration interaction (f.i.s.c.i.).

Downloaded from rsta.royalsocietypublishing.org

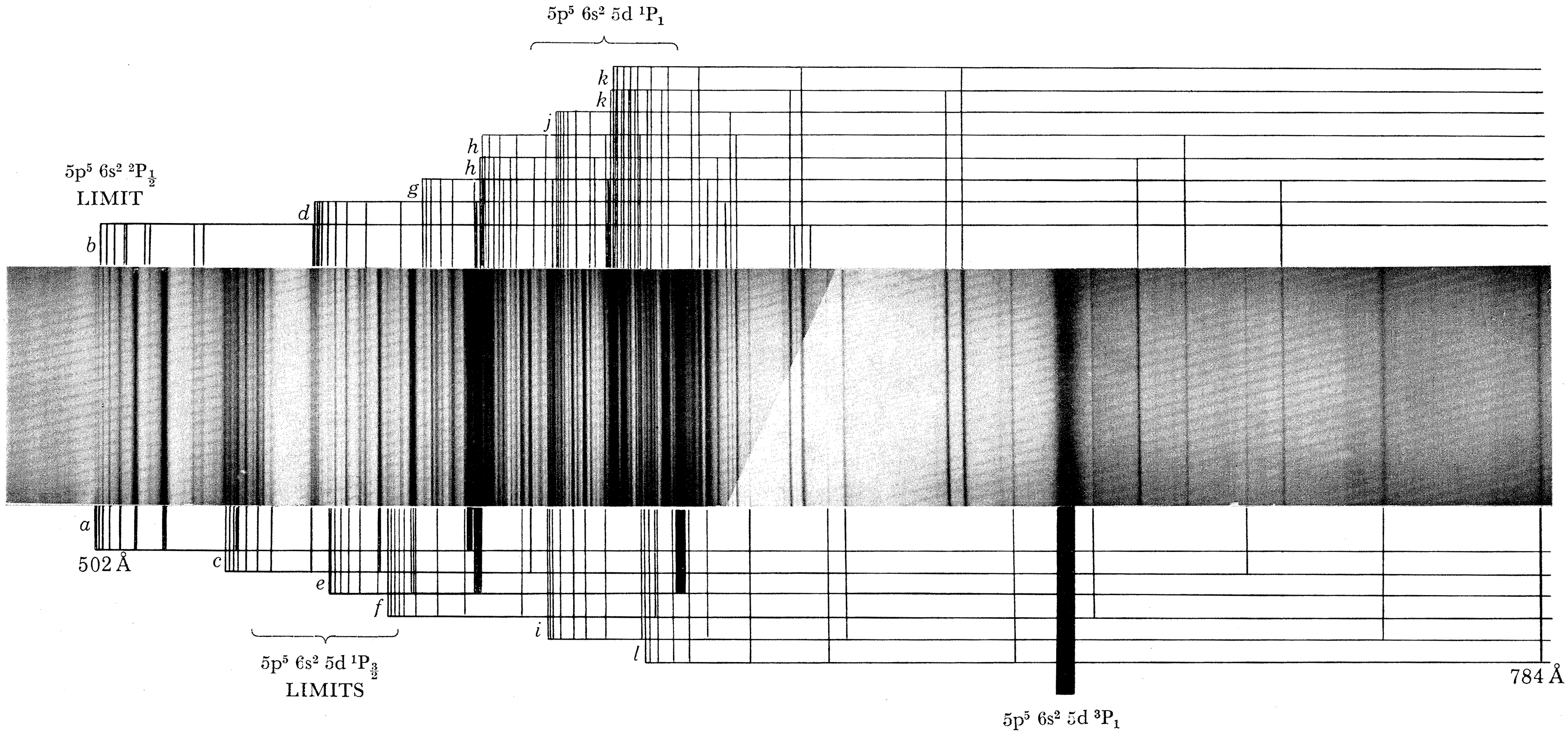

FIGURE 3. The 5p subshell spectrum of Ba I showing how the ordering into Rydberg series is accomplished (after Connerade *et al.* 1979 *a*). From the m.D.–F. calculations, the percentages of $5p^5\,6s^2\,{}^2P$ are associated with limits as follows: *a*, *b*, 79% ${}^2P_{\frac{1}{2}}$; *c*, 10% ${}^2P_{\frac{3}{2}}$; *d*, 41% ${}^2P_{\frac{3}{2}}$; *e*, 24% ${}^2P_{\frac{3}{2}}$; *f*, 2% ${}^2P_{\frac{3}{2}}$; *h*, 2% ${}^2P_{\frac{1}{2}}+6\%\ {}^2P_{\frac{3}{2}}$.

Downloaded from rsta.royalsocietypublishing.org

Inclusion of initial state configuration interaction (i.s.c.i.) does not alter the predicted intensities sufficiently to affect the assignments, and as in the model the ground atomic c.s.f. $[5\bar{\mathrm{p}}^2\,5\mathrm{p}^4\,6\mathrm{s}^2]_0$ is linked to the Ba II c.s.fs $[5\bar{\mathrm{p}}\,5\mathrm{p}^4\,6\mathrm{s}^2]_{\frac{1}{2}}$ $(5\mathrm{p}^5\,6\mathrm{s}^2\,{}^2\mathrm{P}_{\frac{1}{2}})$ and $[5\bar{\mathrm{p}}^2\,5\mathrm{p}^3\,6\mathrm{s}^2]_{\frac{3}{2}}$ $(5\mathrm{p}^5\,6\mathrm{s}^2\,{}^2\mathrm{P}_{\frac{3}{2}})$ only, it is the admixture of these c.s.fs into a particular Ba II level that is found to be the principal factor determining the probability of its production from electron-impact ionization.

Correspondence between the Ba I electron impact 5p-ionization spectrum and the 5p-photoabsorption spectrum (Connerade *et al.* 1979) allows six series limits to be clearly identified. It is supposed that the existence of other series is mainly due to interchannel coupling which is experimentally conspicuous and comparison with the Ba II photoabsorption spectrum of Roig (1976) gives tentative assignments for the remaining series limits.

Our thanks go to Dr F. P. Larkins, Monash University, and Dr K. J. Ross, Southampton University, who both made valuable suggestions at an early stage of the work, and especially to Professor U. Fano, University of Chicago, who instigated our collaboration, as well as to Dr M. W. D. Mansfield of the Culham Laboratory who supplied *LS* coupling energy matrices.

The computations were performed on the IBM 370/195 machine of the Rutherford Laboratory, and the S.R.C. are thanked for the use of this facility and for a maintenance grant for S.J.R.

APPENDIX

In the Appendix we show how equation (4) follows from equation (3) in the text. The transition dipole matrix element between the ground state α and the ionizing state γ with continuum orbital εκ

$$
\begin{aligned}
|d_{z\alpha\gamma}|^2 &= \sum_{M\gamma} |\langle \Psi_\alpha(J_\alpha M_\alpha)|\ \sum_i r_i\, C_0^{(1)}(i)\,|\ \Psi_\gamma(J_\gamma M_\gamma)\rangle|^2 \\
&= |\langle \Psi_\alpha \|\ \sum r_i\, C^{(1)}(i)\, \| \Psi_\gamma\rangle|^2 \times \langle 1010|00\rangle^2 \\
&= \tfrac{1}{3} |\langle \Psi_\alpha \|\ \sum r_i\, C^{(1)}(i)\, \| \Psi_\gamma\rangle|^2,
\end{aligned} \qquad \text{(A 1)}
$$

where the form of the Wigner–Eckart theorem given in equation (4.15) of Brink & Satchler (1968) is used.

By (1) each a.s.f. can be expanded as a linear combination of c.s.fs

$$\Psi_\alpha(J_\alpha M_\alpha) = \sum_{\mathrm{r}} c_{\mathrm{r}\alpha}\, \Phi(\gamma_{\mathrm{r}}\, J_\alpha M_\alpha), \qquad \text{(A 2)}$$

$$\Psi_\gamma(J_\gamma M_\gamma) = \sum_{\mathrm{s}} c_{\mathrm{s}\gamma}\, \Phi(\gamma_{\mathrm{s}}\, J_\gamma M_\gamma), \qquad \text{(A 3)}$$

so

$$|d_{z\alpha\gamma}|^2 = \tfrac{1}{3} |\sum_{\mathrm{r,s}} c_{\mathrm{r}\alpha}\, c_{\mathrm{s}\gamma} \langle \Phi(\gamma_{\mathrm{r}}\, J_\gamma) \|\ \sum_i r_i\, C^{(1)}(i) \|\ \Phi(\gamma_{\mathrm{s}}\, J_\gamma)\rangle|^2. \qquad \text{(A 4)}$$

It is possible to write a reduced matrix element involving a sum of one-electron operators over c.s.fs r and s as a sum of single particle reduced matrix elements

$$\langle \Phi(\gamma_{\mathrm{r}}\, J_\alpha) \|\ \sum_i r_i\, C^{(1)}(i) \|\ \Phi(\gamma_{\mathrm{s}}\, J_\gamma)\rangle = \sum_{a \leqslant b} d_{ab}^{(1)}(\mathrm{r,s})\, \langle a \| \mathrm{r}\, C^{(1)} \| b\rangle. \qquad \text{(A 5)}$$

The coefficients $d_{ab}^{(1)}(\mathrm{r,s})$ are discussed in equations (7)–(12) of Pyper *et al.* (1978) who also present a computer program, developed from that of Chang (1974), which is convenient for their evaluation. From (A 4) and (A 5)

$$|d_{z\alpha\gamma}|^2 = \tfrac{1}{3} |\sum_{\mathrm{r,s}} c_{\mathrm{r}\alpha}\, c_{\mathrm{s}\gamma} \sum_{a \leqslant b} d_{ab}^{(1)}(\mathrm{r,s})\, \langle a \| \mathrm{r}\, C^{(1)} \| b\rangle|^2. \qquad \text{(A 6)}$$

PHILOSOPHICAL TRANSACTIONS OF THE ROYAL SOCIETY A MATHEMATICAL, PHYSICAL & ENGINEERING SCIENCES

PHILOSOPHICAL TRANSACTIONS OF THE ROYAL SOCIETY A MATHEMATICAL, PHYSICAL & ENGINEERING SCIENCES

Downloaded from rsta.royalsocietypublishing.org

MATHEMATICAL, PHYSICAL & ENGINEERING SCIENCES
PHILOSOPHICAL TRANSACTIONS OF THE ROYAL SOCIETY A

With the use of expressions in appendix VI of Brink & Satchler (1968) it is straightforward to prove that

$$\langle a\|r\boldsymbol{C}^{(1)}\|b\rangle = \langle j_a l_a \tfrac{1}{2}\| \boldsymbol{C}^{(1)}\| j_b l_b \tfrac{1}{2}\rangle \int_0^\infty (P_a P_b + Q_a Q_b)\, r\,\mathrm{d}r$$

$$= -\langle j_a \tfrac{1}{2} 1 0 | j_b \tfrac{1}{2}\rangle \int_0^\infty (P_a P_b + Q_a Q_b)\, r\,\mathrm{d}r, \tag{A 7}$$

so that

$$|d_{z\alpha\gamma}|^2 = \tfrac{1}{3}\left|\sum_{\mathrm{r,s}} c_{\mathrm{r}\alpha}\, c_{\mathrm{s}\beta} \sum_{a\leqslant b} d_{ab}^{(1)}(\mathrm{r,s}) \left(-\langle j_a \tfrac{1}{2} 1 0 | j_b \tfrac{1}{2}\rangle \int_0^\infty (P_a P_b + Q_a Q_b)\, r\,\mathrm{d}r\right)\right|^2. \tag{A 8}$$

This can be abbreviated to

$$|d_{z\alpha\gamma}|^2 = \tfrac{1}{3}\Big|\sum_{a\leqslant b} D_{\alpha\gamma}^{\mathrm{ab}} R_{a,b}\Big|^2, \tag{A 9}$$

where

$$D_{\alpha\gamma}^{\mathrm{ab}} = \sum_{\mathrm{rs}} c_{\mathrm{r}\alpha}\, c_{\mathrm{s}\gamma}\, d_{ab}^{(1)}(\mathrm{r,s}) \tag{A 10}$$

and

$$R_{a,b} = -\langle j_a \tfrac{1}{2} 1 0 | j_b \tfrac{1}{2}\rangle \int_0^\infty (P_a P_b + Q_a Q_b)\, r\,\mathrm{d}r. \tag{A 11}$$

The c.s.f. mixing coefficients for the ionizing state γ are taken to be those derived from the calculation on the Ba II ion which is expected to be a fairly good approximation since the coupling between the different ionic channels can only occur through the continuum electron. Thus we take

$$c_{\mathrm{s}\gamma} = c_{\mathrm{s}\beta}, \tag{A 12}$$

which is achieved by replacing γ by β in (3)

$$Q_{\beta\leftarrow\alpha}^{i}(\kappa) \propto \int |d_{z\alpha\beta}(\epsilon\kappa)|^2\, \mathrm{d}\epsilon, \tag{A 13}$$

where it is understood that the label s in $d_{ab}^{(1)}(\mathrm{r,s})$ refers to c.s.fs of the ionizing state γ and not the ionic state β. The initial state consists of c.s.fs with angular momentum structure $([X]_0[j^{2j+1}]_0)_0$ while the final state has the structure $([Y][j^{2j}]_j, j')_1$ and so (from equation (5.20) of Brink & Satchler 1978)

$$\langle([X]_0[j^{2j+1}]_0)_0 \| \sum_i r_i\, \boldsymbol{C}^{(1)}(i)\| ([Y][j^{2j}]_j, j')_1\rangle = (2j+1)^{\frac{1}{2}} \langle j\|r\boldsymbol{C}^{(1)}\|j'\rangle\, \delta_{X,Y}. \tag{A 14}$$

Thus the non-zero coefficients $d_{ab}^{(1)}(\mathrm{r,s})$, table 5, only occur when the c.s.fs r and s have the same parent, $X \equiv Y$, and so equal $(2J_\beta+1)^{\frac{1}{2}}$ independent of the state of the continuum electron. Within the approximation of the model, no Ba II states of $J = \frac{5}{2}$ or $\frac{7}{2}$ will result from the electron impact ionization process, as the relevant coefficients $d_{ab}^{(1)}(\mathrm{r,s})$ must all vanish. Table 5 also shows that for c.s.fs, s, with $J = \frac{1}{2}$ Ba II parentage the 5p̄ orbital is linked to the continuum orbital while for the $J = \frac{3}{2}$ case only the 5p orbital is involved. Consequently

$$|d_{z\alpha\beta}|^2 = \tfrac{1}{3}|\,D_{\alpha\beta}^{\mathrm{e}\kappa} R_{5\mathrm{e},\epsilon\kappa}|^2, \tag{A 15}$$

in which

$$\left.\begin{aligned} \mathrm{e} &= \bar{\mathrm{p}} \quad \text{if} \quad J_\beta = \tfrac{1}{2} \\ \mathrm{e} &= \mathrm{p} \quad \text{if} \quad J_\beta = \tfrac{3}{2} \end{aligned}\right\} \tag{A 16}$$

Downloaded from rsta.royalsocietypublishing.org

MATHEMATICAL, PHYSICAL & ENGINEERING SCIENCES
PHILOSOPHICAL TRANSACTIONS OF THE ROYAL SOCIETY A

where $D^{e\kappa}_{\alpha\beta}$ in (A 15) depends only on the symmetry character of e and κ. With the definitions

$$I_{a,\kappa} = \int |R_{a,\epsilon\kappa}|^2 \, d\epsilon = \langle j_a \tfrac{1}{2} 1 0 | j_\kappa \tfrac{1}{2} \rangle^2 J_a, \tag{A 17}$$

and

$$J_{a,\kappa} = \int \left| \int_0^\infty (P_a P_{\epsilon\kappa} + Q_a Q_{\epsilon\kappa}) \, r \, dr \right|^2 d\epsilon, \tag{A 18}$$

(A 13) gives

$$Q^i_{\beta \leftarrow \alpha} \propto (D^{e\kappa}_{\alpha\beta})^2 I_{5e,\kappa}, \tag{A 19}$$

where e is given by equation (A 16).

The same Ba II level can result from outgoing continuum electrons of different angular character, and contributions from each possible type must be included. The total ionization cross section is then given by

$$\begin{aligned} Q^i_{\beta \leftarrow \alpha} &= \sum_\kappa Q_{\beta \leftarrow \alpha}(\kappa) \\ &\propto \{(D^{es}_{\alpha\beta})^2 I_{5e,s} + (D^{e\bar{d}}_{\alpha\beta}) \, I_{5e,d} + (D^{ed}_{\alpha\beta})^2 I_{5e,d}\}, \end{aligned} \tag{A 20}$$

where the Clebsch–Gordan coefficients in the I integrals limit the number of possible terms. Certain simplifications can be made to (A 20). The values of $d^{(1)}_{ab}(r,s)$ shown in table 5 turn out to be independent of b, and as a consequence (A 20) can be written as

$$Q^i_{\beta \leftarrow \alpha} \propto (D^{e\kappa}_{\alpha\beta})^2 [I_{5e,s} + I_{5e,\bar{d}} + I_{5e,d}], \tag{A 21}$$

where κ may be interpreted as any of s, d̄ or d.

Also since the 5p̄ and 5p orbitals have similar spatial properties and as the J integrals will have a major contribution from continuum orbitals well above threshold then

$$J_{5\bar{p},\kappa} \approx J_{5p,\kappa} \tag{A 22}$$

for each κ, and each integral is roughly independent of the Ba II state β resulting from the ionization. An examination of the values of the Clebsch–Gordan coefficients (listed in table 7) shows that ionization to a $J = \tfrac{1}{2}$ Ba II state can occur in the present model via an ϵs or $\epsilon\bar{d}$ channel and the coefficients for the process are identical in magnitude to those relating to ϵs and ϵd continuum orbitals for $J = \tfrac{3}{2}$ Ba II states. However, the possibility of ionization in the $\epsilon\bar{d}$ channel to a $J = \tfrac{3}{2}$ Ba II level also occurs. Making the reasonable assumption that $\epsilon\bar{d}$ and ϵd orbitals are spatially very similar and from (A 22) then

$$I_{5p,\bar{d}} \approx I_{5p,d} \approx 10 I_{5p,\bar{d}}, \tag{A 23}$$

TABLE 7. CLEBSCH–GORDAN COEFFICIENTS $\langle j_a \tfrac{1}{2} 1 0 | j_b \tfrac{1}{2} \rangle$ APPEARING IN THE SINGLE PARTICLE REDUCED MATRIX ELEMENTS

a	b	j_a	j_b	$\langle j_a \tfrac{1}{2} 10 \| j_b \tfrac{1}{2} \rangle$
5p̄	ns	$\tfrac{1}{2}$	$\tfrac{1}{2}$	$\frac{1}{\sqrt{3}}$
5p	ns	$\tfrac{3}{2}$	$\tfrac{1}{2}$	$\frac{-1}{\sqrt{3}}$
5p̄	nd̄	$\tfrac{1}{2}$	$\tfrac{3}{2}$	$\sqrt{\tfrac{2}{3}}$
5p	nd̄	$\tfrac{3}{2}$	$\tfrac{3}{2}$	$\frac{1}{\sqrt{15}}$
5p	nd	$\tfrac{3}{2}$	$\tfrac{5}{2}$	$-\sqrt{\tfrac{2}{3}}$

Downloaded from rsta.royalsocietypublishing.org

PHILOSOPHICAL TRANSACTIONS OF THE ROYAL SOCIETY A MATHEMATICAL, PHYSICAL & ENGINEERING SCIENCES

PHILOSOPHICAL TRANSACTIONS OF THE ROYAL SOCIETY A MATHEMATICAL, PHYSICAL & ENGINEERING SCIENCES

the factor of 10 arising from the Clebsch–Gordan coefficient. Thus, ignoring the relatively small $I_{5\mathrm{p},\bar{\mathrm{d}}}$ contribution,

$$Q^{i}_{\beta\leftarrow\alpha} \propto \begin{cases} (D^{\bar{\mathrm{p}}\kappa}_{\alpha\beta})^2[I_{5\bar{\mathrm{p}},\mathrm{s}}+I_{5\bar{\mathrm{p}},\bar{\mathrm{d}}}], & J_\beta = \frac{1}{2} \\ (D^{\mathrm{p}\kappa}_{\alpha\beta})^2[I_{5\mathrm{p},\mathrm{s}}+I_{5\mathrm{p},\mathrm{d}}], & J_\beta = \frac{3}{2} \end{cases} \tag{A 24}$$

and from (A 22) and (A 23) we conclude

$$Q^{i}_{\beta\leftarrow\alpha} \propto (D^{\mathrm{e}\kappa}_{\alpha\beta})^2, \tag{A 25}$$

which is equation (4) of the text.

REFERENCES

Beutler, H. & Guggenheimer, K. 1934 *Z. Phys.* **88**, 25.

Brehm, B. & Bucher, A. 1974 *Int. J. Mass Spectrum. Ion Phys.* **15**, 463.

Brink, D. M. & Satchler, G. R. 1968 *Angular momentum*. Oxford: Clarendon Press.

Chang, J. J. 1974 *Computer Phys. Communs.* **7**, 223.

Connerade, J. P. 1970 *Astrophys. J.* **159**, 685.

Connerade, J. P. & Mansfield, M. W. D. 1974 *Proc. R. Soc. Lond.* A **341**, 267.

Connerade, J. P. & Mansfield, M. W. D 1978, private communication.

Connerade, J. P., Mansfield, M. W. D., Newsom, G. H., Tracy, D. H., Baig, M. A. & Thimm, K. 1979*a* *Phil. Trans. R. Soc. Lond.* A **290**, 327.

Connerade, J. P., Mansfield, M. W. D., Thimm, K. & Tracy, D. H. 1974 *Vacuum ultraviolet radiation physics* (ed. Koch, E. E., Haensal, R. & Kunz, C.), pp. 99, 235. Braunschweig: Vieweg/Pergamon.

Connerade, J. P., Rose, S. J. & Grant, I. P. 1979*b* *J. Phys.* B **12**, L53.

Connerade, J. P. & Tracy, D. H. 1977 *J. Phys.* B **10**, L235.

Fano, U. 1973 *Comments atom. molec. Phys.* **4**, 128.

Grant, I. P., Mayers, D. M. & Pyper, N. C. 1976 *J. Phys.* B **9**, 2777.

Hansen, J. 1974 *J. Phys.* B **7**, 1902.

Hansen, J. 1975*a* *J. Phys.* B **8**, L403.

Hansen, J. 1975*b* *J. Phys.* B **8**, 2759.

Hotop, H. & Mahr, D. 1975 *J. Phys.* B **8**, L301.

Hultzch, W., Kronast, W., Niehaus, A. & Ruf, M. W. 1979 *J. Phys.* B **12**, 1821.

Martin, R. L. & Shirley, D. A. 1976 *J. chem. Phys.* **64**, 3685.

Mehlhorn, W., Breuckmann, B. & Hausamann, D. 1977 *Physica Scri.* **16**, 177.

Mitchell, P. 1979 *J. Phys.* B **12**, 1653.

Mott, N. F. & Massey, H. S. W. 1965 *The theory of atomic collisions*. Oxford: Clarendon Press.

Potts, A. W. & Lee, E. P. F. *J. Phys.* B **12**, L413.

Pyper, N. C., Grant, I. P. & Beatham, N. 1978 *Computer Phys. Communs* **15**, 387.

Roig, R. A. 1976 *J. opt. Soc. Am.* **66**, 1400.

Rose, S. J., Pyper, N. C. & Grant, I. P. 1978 *J. Phys.* B **11**, 755.

Wendin, G. 1974 *Vacuum ultraviolet radiation physics* (ed. Koch, E. E., Haensal, R. & Kunz, C.), p. 235. Braunschweig: Vieweg/Pergamon.

Wendin, G. 1978 *Daresbury Laboratory Report* DL/SCI/R11 (Proceedings of one day meeting on Photoionization of Atoms and Molecules, 16 February 1978).

NOTES ADDED IN PROOF

1. In a recent paper (Mitchell 1979) published since part I of this investigation, it is suggested that the assignment of $5\mathrm{p}^5 6\mathrm{s}^2\ {}^2\mathrm{P}_{\frac{1}{2}}$ of CsI given by Beutler & Guggenheimer (1933) for the level at 109069 cm^{-1} is incorrect and the ${}^2\mathrm{P}_{\frac{1}{2}}$ level must be higher in energy. The same conclusion was reached independently in our earlier paper. (Connerade *et al.* 1979*a*) but corrected in a different way. Mitchell (1979) suggests that 111500 cm^{-1} should be assigned $5\mathrm{p}^5 6\mathrm{s}^2\ {}^2\mathrm{P}_{\frac{1}{2}}$ and that 109069 cm^{-1} ‘presumably belongs to the configuration $5\mathrm{p}^5 6\mathrm{s}5\mathrm{d}$’. We assigned 113488 cm^{-1} as $5\mathrm{p}^5 6\mathrm{s}^2\ {}^2\mathrm{P}_{\frac{1}{2}}$ because it is the only appropriate intense transition in the optical spectrum, and we have identified several $5\mathrm{p}^5 5\mathrm{d}6\mathrm{s}$ levels among which $5\mathrm{p}^5 5\mathrm{d}({}^3\mathrm{P})6\mathrm{s}\ {}^2\mathrm{P}_{\frac{3}{2}}$ at 109150 cm^{-1}.

2. Hultzch *et al.* (1979) have observed the autoionization spectrum of Ba following impact excitation by He$^+$ and Ne$^+$. Although there is a good correspondence between the 1000 eV He$^+$ spectrum and the electron impact spectrum, the detailed assignments which they report differ from the present ones.

In this connection we also draw attention to a recent letter on the 5p photoelectron spectrum by Potts & Lee (1979) whose results appear to confirm the present analysis.

Downloaded from rsta.royalsocietypublishing.org

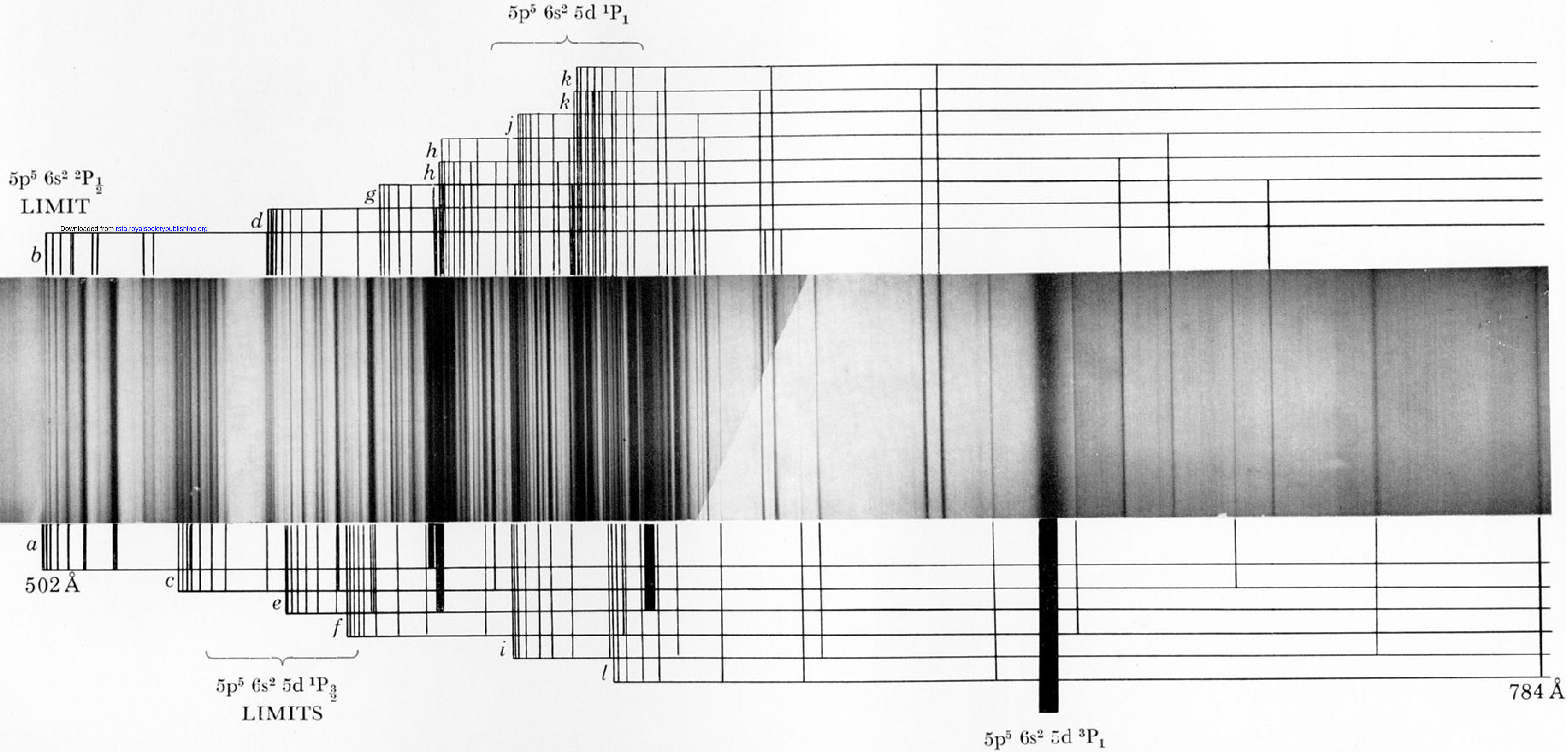

FIGURE 3. The 5p subshell spectrum of Ba I showing how the ordering into Rydberg series is accomplished (after Connerade *et al.* 1979*a*). From the m.D.–F. calculations, the percentages of $5p^5\ 6s^2\ ^2P$ are associated with limits as follows: *a*, *b*, 79% $^2P_{\frac{1}{2}}$; *c*, 10% $^2P_{\frac{3}{2}}$; *d*, 41% $^2P_{\frac{3}{2}}$; *e*, 24% $^2P_{\frac{3}{2}}$; *f*, 2% $^2P_{\frac{3}{2}}$; *h*, 2% $^2P_{\frac{1}{2}} + 6\%\ ^2P_{\frac{3}{2}}$.